

Resonant-Collision Spectroscopy of Rydberg Atoms

R. C. Stoneman, M. D. Adams,^(a) and T. F. Gallagher

Department of Physics, University of Virginia, Charlottesville, Virginia 22901

(Received 22 December 1986)

Resonant collisional energy transfer between atoms with small relative velocity is shown to have such long collision times, $\sim 0.17 \mu\text{s}$, or equivalently such narrow linewidths, 6 MHz, that it may be used to make spectroscopic measurements. Specifically, we report the use of the sharply resonant collisional energy transfer $ns + (n-2)d \rightarrow np + (n-1)p$ between velocity-selected K atoms to determine an improved value, 1.711 925(5), of the K np -state quantum defect.

PACS numbers: 34.60.+z, 32.60.+i

Collisions are normally avoided in precision spectroscopy, since their presence tends to broaden the spectral features of interest. In a few high-resolution studies, however, collisions have been crucial to the success of the experiment.¹⁻³ For example, hydrogen-deuterium spin-exchange collisions have been used to couple the polarizations of H and D in a hydrogen maser weakly, allowing the D hyperfine transition to be observed as a change in the output of the maser.² In all such spectroscopic uses the collision was not the high-resolution probe itself, but only a state selector or detector. Here we report what is to our knowledge the first use of a collision process as the high-resolution spectroscopic probe. That is, the spectroscopic resolution is limited by the collision time, just as the microwave interaction time provides the resolution limit in the maser experiment. Specifically, we have used resonant collisional energy transfer between highly excited K atoms to measure the quantum defect of the p state of K with significantly improved precision.

Resonant collisional energy transfer between two atoms occurs through the dipole-dipole interaction, with strength $\mu_1\mu_2/r^3$, where μ_1 and μ_2 are the dipole matrix elements connecting the initial and final states of the two atoms, and r is the separation of the two atoms. When two atoms collide, collisional energy transfer is probable if the interaction strength integrated over the collision time is approximately 1. For a collision with impact parameter b this reduces to $(\mu_1\mu_2/b^3)(b/v) = 1$, where v is the collision velocity.⁴⁻⁶ This leads immediately to expressions for the cross section,

$$\sigma \approx b^2 = \mu_1\mu_2/v, \quad (1)$$

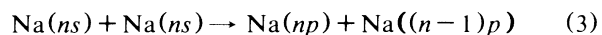
and the collision time,

$$t = b/v = (\mu_1\mu_2)^{1/2}/v^{3/2}, \quad (2)$$

both in atomic units.

If the colliding atoms are Rydberg atoms of principal quantum number n , and the dipole transitions are to the adjacent dipole-allowed levels, then $\mu_1 \approx \mu_2 \approx n^2$, $\sigma \approx n^4/v$, and $t \approx n^2/v^{3/2}$. For thermal velocity ($v \sim 3 \times 10^{-4}$) collisions between $n=20$ atoms, the predicted

cross sections and collision times are 10^8 \AA^2 and 10^{-9} s, respectively. The surprisingly large magnitudes of these cross sections and collision times, as well as their n dependences, have been confirmed by Safinya *et al.*,⁴ who studied the process



which is resonant when the Na energy levels are tuned with an electric field such that the ns level lies halfway between the np and $(n-1)p$ levels.

From a spectroscopic point of view, a collision time of 1 ns, or a collisional resonance linewidth of 1 GHz, is roughly the resolution obtained in a Doppler-broadened absorption spectrum, but it is not at all comparable to the ~ 1 -MHz resolution of Doppler-free two-photon spectroscopy. However, Eq. (2) implies that a smaller collision velocity leads to a reduction in linewidth. If the collision velocity is made small enough, precise spectroscopic measurements become possible. For the measurements described here, we have used velocity-selected K atoms, resulting in collisional resonances as narrow as 6 MHz.

Specifically, we have studied the resonant collision process



which occurs when the levels are shifted into resonance with a small electric field F . The relevant energy levels, for $n=29$, are shown in Fig. 1. At resonance the $29p$ - $29s$ and $27d$ - $28p$ intervals are equal; i.e., the quantity

$$W(F) = [E_{np}(F) + E_{(n-1)p}(F)] - [E_{ns}(F) + E_{(n-2)d}(F)] \quad (5)$$

is zero at resonance. In Eq. (5), $E_{np}(F)$, for example, is the energy of the np state in an electric field F . In Fig. 1 the process $29s \rightarrow 29p$, $27d \rightarrow 28p$ is shown. The complementary process $29s \rightarrow 28p$, $27d \rightarrow 29p$ is not shown in the figure. The two processes are not resolved experimentally, since the resonance fields are identical for the two processes, as can be seen by Eq. (5). Because of the similarity of the two processes, their cross sections are

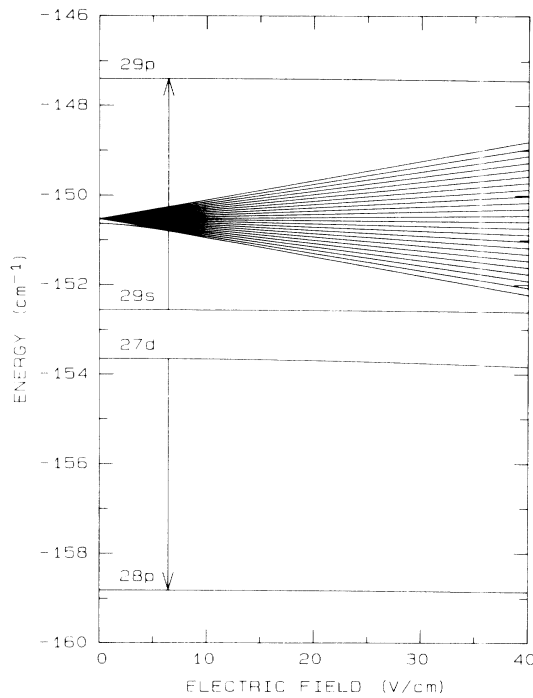


FIG. 1. Energy levels for the resonant collision of $29s$ and $27d$ atoms. The collision process $29s \rightarrow 29p$, $27d \rightarrow 28p$ is indicated by the arrows. For clarity, the complementary process $29s \rightarrow 28p$, $27d \rightarrow 29p$ is not shown. The $n=27$ linear Stark levels are included for reference.

expected to be very nearly equal. The resonance measurements, performed in weak electric fields, allow us to determine the energies of the np states relative to the ns and nd state energies which are known to high precision from Doppler-free two-photon spectroscopy.

In the experiment an atomic beam of potassium passes between two field plates 1.590(1) cm apart where the atoms are excited from the $4s$ ground state to the $4p_{1/2}$ state by a pulsed tunable laser of wavelength 770 nm, and then to the $29s_{1/2}$ and $27d_{3/2}$ levels by two more pulsed lasers at wavelengths ≈ 457 nm. The excited atoms are allowed to collide with each other for 1 μ s after excitation and are then field ionized by a high-voltage pulse. The pulse is large enough to ionize the $29p$ state but not the $29s$, $27d$, or $28p$ states. The ions produced pass through 0.4-mm-diam holes in the upper plate to a particle multiplier, and the resulting signal is recorded with a gated integrator. The collisional resonance signal is observed as a substantial increase in the $29p$ signal as the static field is scanned through the collisional resonance at 6.43 V/cm. The resonance signal is observed to disappear when either of the blue lasers is blocked, demonstrating that the signal is indeed due to the process of Eq. (4). There is, however, a small non-resonant background np signal present when either blue laser is blocked, due to excitation of atoms from the $29s$ and $27d$ states to the $29p$ state by 300-K blackbody radi-

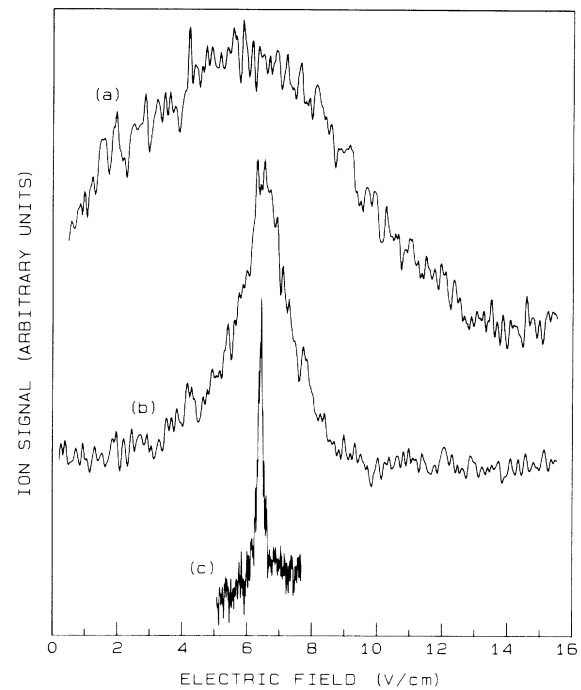


FIG. 2. Observed collisional resonances for $29s$. Spectrum (a) is produced by atoms in a cell, (b) by atoms in a beam, and (c) by atoms in a velocity-selected beam. The asymmetry evident in (a) and (b) disappears when the spectra are plotted vs the square of the field (i.e., vs energy).

ation.⁷

The electric fields used in these experiments are low enough that the j, m_j quantum numbers provide a good description of both the np and nd states. Thus by polarizing both laser beams parallel to the static electric field, and using the $4p_{1/2}$ intermediate state, we excite only the $nd_{3/2}$, $|m_j| = \frac{1}{2}$ levels. Other combinations of intermediate state and laser polarizations lead to the excitation of different states and hence different collisional resonances.⁸

In Fig. 2 we show scans of the $n=29$ resonance of Fig. 1 under several conditions. The broad resonance in Fig. 2(a) is due to collisions between pairs of atoms whose relative velocities are oriented randomly. Although the atoms are emitted from the oven in a beam, they subsequently bounce from the room-temperature walls of the vacuum chamber, effectively converting the chamber into a cell of K atoms with velocities in random directions. To obtain Fig. 2(b) the interaction region is surrounded by a trap cooled with liquid nitrogen. Under these conditions K atoms stick to the trap, and the resonance signal is due solely to collisions between atoms in the beam, which are all moving in the same direction. The average relative atomic velocity is smaller for the one-dimensional modified Maxwellian distribution of the beam than for the three-dimensional distribution of the cell. This accounts for the narrowness of the resonance

(b) relative to (a). The asymmetry evident in both (a) and (b) is not surprising, since the resonances are expected to be symmetric with respect to energy, and the Stark shifts are quadratic in the field. In fact these resonances are symmetric when plotted versus the square of the electric field.

The spectrum of Fig. 2(c) is produced by collisions between atoms in a velocity-selected beam. The velocity selection is achieved by our placing a chopper wheel between the oven and the interaction region. The wheel has radius 4.8 cm, and rotates at 200 Hz. A 0.15-cm-wide slot is cut into the wheel, producing a pulse of atoms with duration $\tau = 25 \mu\text{s}$. The distance, d , from the wheel to the interaction region is 14 cm. The laser is synchronized with the chopper by detection of the slot with a light-emitting diode and photodiode. The delay, T , from the opening of the slot to the firing of the laser is typically $250 \mu\text{s}$. The velocity spread at the interaction region is

$$\Delta v = (\tau/T)d/(T - \tau). \quad (6)$$

Given the above parameters, the velocity spread of the selected atoms is $1 \times 10^4 \text{ cm/s}$.

The resonance fields and widths for the spectra of Fig. 2 are given in Table I. These parameters are obtained from a least-squares fit of the data by a Lorentzian line shape, where the independent variable is the square of the electric field. The widths (in units of field squared) are converted to frequency widths by multiplication by A , where $W(F) = AF^2$ (i.e., twice the net polarizability of the levels involved in the collision). The coefficient A is calculated by numerical diagonalization of the energy matrix,⁹ and is found to be $2.46 \text{ MHz}/(\text{V/cm})^2$ for $n = 29$.

The velocity-selected collisional resonance

$$ns_{1/2} + (n-2)d_{3/2} \rightarrow np_{1/2} + (n-1)p_{1/2}$$

was observed for three values of n , and the resonance fields are given in Table II. At these fields the average energy of the $np_{1/2}$ and $(n-1)p_{1/2}$ states equals the average energy of the $ns_{1/2}$ and $(n-2)d_{3/2}$ states, and by taking into account the small Stark shifts we can easily determine the zero-field np quantum defects from the ns and nd quantum defects.

The n dependence of the quantum defect, δ_l , of the center of gravity of the nl state can be represented by an

extended Ritz formula

$$\delta_l = \delta_l^0 + \delta_l^1(n^*)^{-2} + \delta_l^2(n^*)^{-3}. \quad (7)$$

Two-photon Doppler-free spectroscopy has been used to determine the quantum-defect coefficients for the K s and d states.¹⁰ The coefficients are $\delta_s^0 = 2.180335(7)$, $\delta_s^1 = 5.307(20)$, and for the d states $\delta_d^0 = 0.277072(3)$, $\delta_d^1 = -1.02350(7)$, and $\delta_d^2 = -0.9109(18)$. Similarly, the n dependence of the fine-structure splitting S_l can be represented by

$$S_l = A_l(n^*)^{-3} + B_l(n^*)^{-5} + C_l(n^*)^{-7}. \quad (8)$$

For the K d states, radio-frequency spectroscopy has been used to find $A_l = -37.84(2) \text{ cm}^{-1}$, $B_l = -480.7(23) \text{ cm}^{-1}$, and $C_l = 2417(77) \text{ cm}^{-1}$ for the fine-structure coefficients.¹¹

Risberg¹² has measured the K p -state energies for n in the range 4 to 10 and fitted each of the observed fine-structure series separately by Eq. (7). A better procedure, however, is to fit the center of gravity of the observed energies by Eq. (7), and the fine-structure splittings by Eq. (8). By use of Risberg's data, this procedure yields $\delta_p^0 = 1.71179(12)$, $\delta_p^1 = 0.233(3)$, and $\delta_p^2 = 0.19(1)$. Recent radio-frequency resonance measurements¹³ have found $S_p(n=28) = 1104.26(6) \text{ MHz}$ and $S_p(n=29) = 987.35(4) \text{ MHz}$. These measurements, together with Risberg's values, give $A_p = 669.49(4) \text{ cm}^{-1}$, $B_p = -226(25) \text{ cm}^{-1}$, and $C_p = 435(130) \text{ cm}^{-1}$. The coefficient A_p is determined primarily by the high- n measurements, while B_p and C_p are determined primarily by the low- n measurements. Similarly, a much improved value for the coefficient δ_p^0 can be obtained from the $n = 27, 28$, and 29 resonant collision measurements, while the coefficients δ_p^1 and δ_p^2 determined from Risberg's data have little effect on the high- np -state energies.

As a first step in determining the improved δ_p^0 value, the Stark shift $W(F_0) - W(0)$, where F_0 is the measured resonant collision field, is calculated by numerical diagonalization⁹ of the energy matrix with use of the value of δ_p^0 from Risberg's data. The basis set for this calculation is taken to be all of the states from three quantum numbers below to three quantum numbers above the states involved in the collision. A new value of δ_p^0 was immediately obtained from the calculated Stark shift. This procedure was repeated, with the improved

TABLE I. Resonance fields and width for the spectra shown in Fig. 2.

| Figure | Field (V/cm) | FWHM (MHz) |
|--------|--------------|------------|
| 2(a) | 6.5(4) | 240(30) |
| 2(b) | 6.54(15) | 57(5) |
| 2(c) | 6.43(2) | 5.8(5) |

TABLE II. Observed resonance fields, and the p -state quantum defects derived from them.

| State | Field (V/cm) | δ_p^0 |
|-------|--------------|--------------|
| 29s | 6.43 | 1.711924 |
| 28s | 17.74(4) | 1.711924 |
| 27s | 29.71(4) | 1.711927 |

δ_p^0 value replacing the Risberg value in the diagonalization calculation. However, this refinement proved to be unnecessary, since the Stark shift is approximately independent of δ_p^0 . In Table II we give the resulting δ_p^0 values for the observed resonances.

The sources of uncertainty in the determination of δ_p^0 include the calculation of the Stark shifts, the precision of the s - and d -state quantum defects and the p - and d -state fine structures, and the precision of the measured collisional resonance fields. Interestingly, the dominant uncertainty is from the s and d quantum defects, not from the collisional resonances. In total we are able to give as the value for the p -state quantum defect

$$\delta_p^0 = 1.711925(5).$$

In conclusion we have shown that resonant dipole-dipole collisional energy exchange between atoms with small relative velocity can occur with long collision times, which allows one to use and study collisions in new ways. To demonstrate this we have used such collisions to make a 25-fold improvement in precision over the previous value of the quantum defect of the K np states.

It is a pleasure to acknowledge useful discussions with L. A. Bloomfield, G. Janik, and D. J. Larson, and the

support of the U.S. Air Force Office of Scientific Research under Grant No. AFOSR-87-0007.

^(a)Present address: University of Colorado, Boulder, CO 80309.

¹H. G. Dehmelt, Phys. Rev. **109**, 381 (1958).

²S. B. Crampton, H. G. Robinson, D. Kleppner, and N. F. Ramsey, Phys. Rev. **141**, 55 (1966).

³W. H. Wing, G. A. Ruff, W. E. Lamb, Jr., and J. J. Spezeski, Phys. Rev. Lett. **36**, 1488 (1976).

⁴K. A. Safinya, J. F. Delpech, F. Gounand, W. Sandner, and T. F. Gallagher, Phys. Rev. Lett. **47**, 405 (1981).

⁵T. F. Gallagher, K. A. Safinya, F. Gounand, J. F. Delpech, W. Sandner, and R. Kachru, Phys. Rev. A **25**, 1905 (1982).

⁶N. F. Mott and H. S. W. Massey, *The Theory of Atomic Collisions* (Clarendon, Oxford, 1950).

⁷T. F. Gallagher and W. E. Cooke, Phys. Rev. Lett. **42**, 835 (1979).

⁸R. C. Stoneman and T. F. Gallagher, unpublished.

⁹M. L. Zimmerman, M. G. Littman, M. M. Kash, and D. Kleppner, Phys. Rev. A **20**, 2251 (1979).

¹⁰D. C. Thompson, M. S. O'Sullivan, B. P. Stoicheff, and Gen-Xing Xu, Can. J. Phys. **61**, 949 (1983).

¹¹T. F. Gallagher and W. E. Cooke, Phys. Rev. A **18**, 2510 (1978).

¹²P. Risberg, Ark. Fys. **10**, 583 (1956).

¹³R. C. Stoneman and T. F. Gallagher, unpublished.